JCI The Journal of Clinical Investigation

Thioredoxin-like 2 regulates human cancer cell growth and metastasis via redox homeostasis and NF-κB signaling

Ying Qu, … , Ning-Hui Cheng, Xiaojiang Cui

J Clin Invest. 2011;121(1):212-225. https://doi.org/10.1172/JCI43144.

Research Article **Oncology**

Cancer cells have an efficient antioxidant system to counteract their increased generation of ROS. However, whether this ability to survive high levels of ROS has an important role in the growth and metastasis of tumors is not well understood. Here, we demonstrate that the redox protein thioredoxin-like 2 (TXNL2) regulates the growth and metastasis of human breast cancer cells through a redox signaling mechanism. TXNL2 was found to be overexpressed in human cancers, including breast cancers. Knockdown of TXNL2 in human breast cancer cell lines increased ROS levels and reduced NF-κB activity, resulting in inhibition of in vitro proliferation, survival, and invasion. In addition, TXNL2 knockdown inhibited tumorigenesis and metastasis of these cells upon transplantation into immunodeficient mice. Furthermore, analysis of primary breast cancer samples demonstrated that enhanced TXNL2 expression correlated with metastasis to the lung and brain and with decreased overall patient survival. Our studies provided insight into redox-based mechanisms underlying tumor growth and metastasis and suggest that TXNL2 could be a target for treatment of breast cancer.

Thioredoxin-like 2 regulates human cancer cell growth and metastasis via redox homeostasis and NF-κB signaling

Ying Qu,[1,2] Jinhua Wang,[2] Partha S. Ray,[3] Hua Guo,[4] Jian Huang,[5] Miyung Shin-Sim,[6] Bolanle A. Bukoye,[7] Bingya Liu,[1] Adrian V. Lee,[5] Xin Lin,[8] Peng Huang,[9] John W. Martens,[10] Armando E. Giuliano,[3] Ning Zhang,[4] Ning-Hui Cheng,[7] and Xiaojiang Cui[2]

[1]Department of Surgery, Ruijin Hospital, Institute of Digestive Surgery, Shanghai Jiaotong University School of Medicine, Shanghai, China. [2]Department of Molecular Oncology and [3]Department of Surgical Oncology, John Wayne Cancer Institute, Santa Monica, California, USA. [4]Center for Basic Medical Sciences, Tianjin Medical University, Tianjin, China. [5]Breast Center and Department of Medicine, Baylor College of Medicine, Houston, Texas, USA. [6]Department of Biostatistics, John Wayne Cancer Institute, Santa Monica, California, USA. [7]USDA/ARS Children's Nutrition Research Center and Department of Pediatrics, Baylor College of Medicine, Houston, Texas, USA. [8]Department of Molecular and Cellular Oncology and [9]Department of Molecular Pathology, University of Texas MD Anderson Cancer Center, Houston, Texas, USA. [10]Department of Medical Oncology, Erasmus Medical Center, Josephine Nefkens Institute, Rotterdam, The Netherlands.

Cancer cells have an efficient antioxidant system to counteract their increased generation of ROS. However, whether this ability to survive high levels of ROS has an important role in the growth and metastasis of tumors is not well understood. Here, we demonstrate that the redox protein thioredoxin-like 2 (TXNL2) regulates the growth and metastasis of human breast cancer cells through a redox signaling mechanism. TXNL2 was found to be overexpressed in human cancers, including breast cancers. Knockdown of TXNL2 in human breast cancer cell lines increased ROS levels and reduced NF-κB activity, resulting in inhibition of in vitro proliferation, survival, and invasion. In addition, TXNL2 knockdown inhibited tumorigenesis and metastasis of these cells upon transplantation into immunodeficient mice. Furthermore, analysis of primary breast cancer samples demonstrated that enhanced TXNL2 expression correlated with metastasis to the lung and brain and with decreased overall patient survival. Our studies provided insight into redox-based mechanisms underlying tumor growth and metastasis and suggest that TXNL2 could be a target for treatment of breast cancer.

Introduction

ROS, including superoxide O^{-2}, hydroxyl radical OH, and H_2O_2, are constantly generated during intracellular metabolism and in response to environmental stimuli (1). Generally, ROS are regarded as host-defending molecules that destroy exogenous pathogens (2) and act as secondary messengers in signal transduction (1, 3). However, increased production of ROS is involved in committing cells to apoptosis (3, 4). Although ROS are involved in tumorigenesis and progression, as reflected by ROS activation of tumor-promoting signaling pathways (5), excess oxidative stress, due to further elevated ROS levels beyond a threshold or weakened antioxidative defense, can damage macromolecules vital for cellular functions (6, 7). This in turn results in pathophysiological changes, such as apoptosis, cell cycle disruption, and necrosis (8). As such, induction of ROS-mediated damage in cancer cells by proper pharmacological agents that either promote ROS generation or disable the cellular antioxidant system has been considered as a "radical" therapeutic strategy to preferentially kill cancer cells (9).

The redox state in the normal cell is balanced by the cellular antioxidant capacity to maintain a viable steady-state environment that is predominantly reducing (10). A key mechanism by which cells regulate redox processes is the reversible formation of disulfides through the oxidation of thiol groups in cysteine residues (11). To maintain the cellular thiol-disulfide redox balance, living cells possess 2 major regulatory systems: the thioredoxin/thioredoxin (Trx/Trx) reductase system and the glutaredoxin/glutathione/glutathione (Grx/GSH/GSH) reductase system (12). Trx-1 (12 kDa) is a well-documented member of the Trx regulatory system that reduces disulfide bonds and thus regulates the activity of transcriptional factors like AP-1, NF-κB, and p53 (13, 14). Overexpression of Trx-1 inhibits apoptosis (15). Grxs can readily reduce S-glutathionylated protein (protein-SSG) mixed disulfide and can be regenerated by the reduced form of GSH (16). Grxs protect cells against oxidative stress by catalyzing protein de-glutathionylation and has therefore been implicated in various cellular processes, including regulation of transcription factor binding activities and redox regulation (17–19). For example, Grx-1 regulates intracellular and extracellular homeostasis of protein glutathionylation (20–22).

Elevated oxidative status has been observed in many types of cancer cells, due in part to their high metabolic rate. On the other hand, many tumor cells possess stronger antioxidative defense mechanisms to counterbalance excessive ROS, maintain their redox status, and thus suppress apoptosis (23). This phenomenon may be a consequence of cellular adaption to ROS stress and may play an important role in the development of highly malignant behaviors and drug resistance (9). Overexpression of Trx-1 in MCF-7 human breast cancer cells enhances cell growth (24). Increased Trx-1 protein levels are found in several human cancers (25, 26). Interestingly, Grx-1 expression can be induced by oxidative stress in breast cancer cells and thus inhibits apoptosis (27).

During a recent microarray analysis of the IGF-regulated genes in breast cancer cells, we found that a novel Trx-related protein, Trx-like 2

Authorship note: Ying Qu and Jinhua Wang contributed equally to this work.
Conflict of interest: The authors have declared that no conflict of interest exists.
Citation for this article: *J Clin Invest.* 2011;121(1):212–225. doi:10.1172/JCI43144.

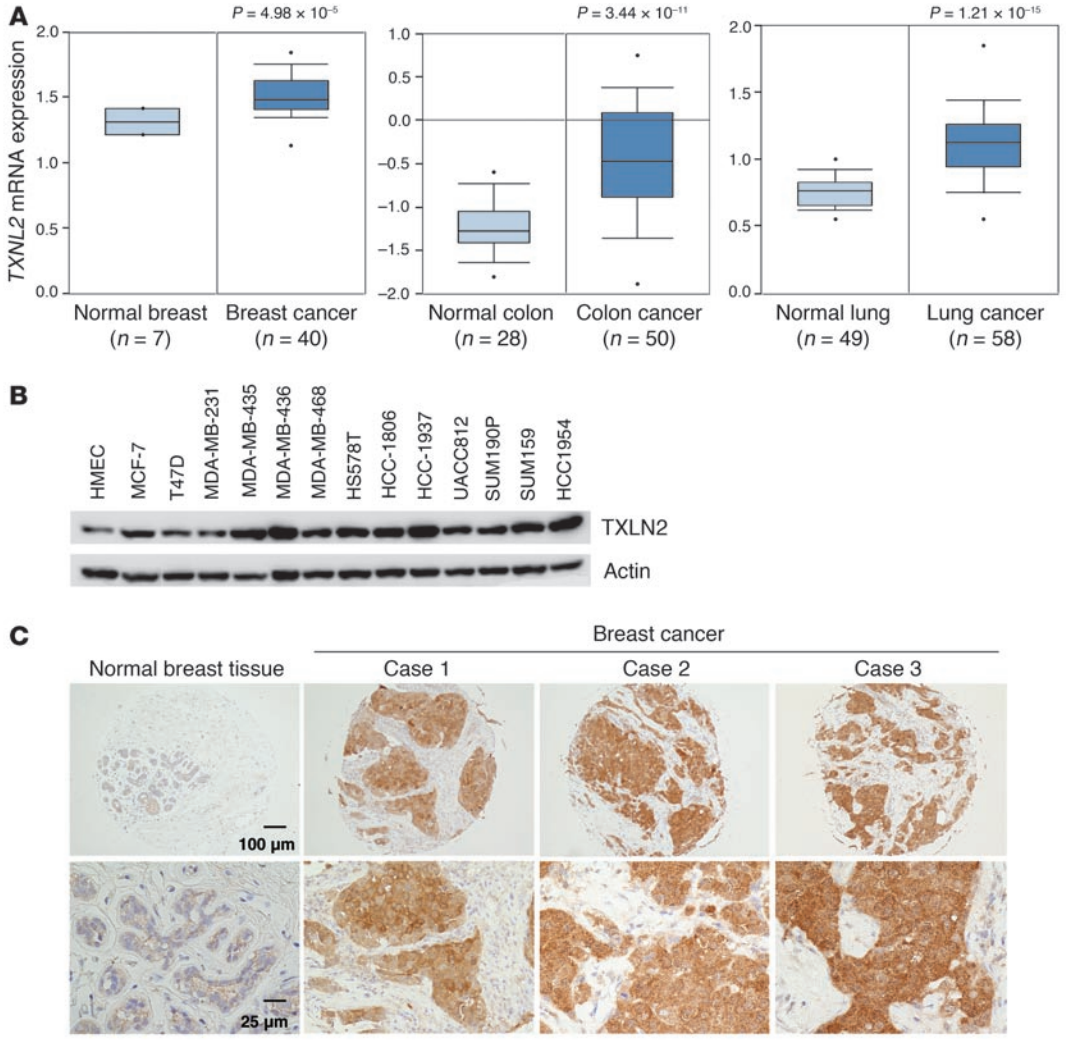

Figure 1

Expression of TXNL2 in human cancers and breast cancer tissues/cell lines. (**A**) Microarray data analyses of TXNL2 expression in human cancers are shown. *TXNL2* mRNA levels in human normal/cancer tissues (breast [ref. 35], colon [ref. 37], and lung [ref. 36]) are plotted. The Student *t* test was conducted using the Oncomine software. The boxes represent the 25th through 75th percentiles. The horizontal lines represent the medians. The whiskers represent the 10th and 90th percentiles, and the asterisks represent the end of the ranges. (**B**) Expression of TXNL2 in normal human breast epithelial cells (HMECs) and 13 breast cancer cell lines was examined using Western blotting. β-Actin was used as a loading control. (**C**) Immunohistochemistry of TXNL2 on tissue microarrays containing normal breast and breast cancer tissues. Low-magnification (top; original magnification, ×100) and high-magnification (bottom; original magnification, ×400) images of representative staining are shown.

(TXNL2; also known as Grx3 and PICOT), is significantly induced by IGFs (28). The 38-kDa TXNL2 protein is much larger than typical Trx proteins and has a unique protein structure consisting of an N-terminal Trx homology region, followed by 2 tandem repeats of Grx domains (22, 29, 30). Grx3/4, the yeast homolog of TXNL2, was implicated in the regulation of the oxidative stress response (31). Although TXNL2 is conserved in eukaryotes, the physiological function in mammalian cells is still poorly understood (30). Recent reports showed that it can inhibit cardiac hypertrophy through enhancing ventricular function and cardiomyocyte contractility and can regulate FcεRI-mediated mast cell activation (32, 33). Deletion of TXNL2 in mice causes embryonic lethality (34), indicating its role in protecting cells against oxidative stress during embryogenesis.

We hypothesized that TXNL2 may play an important role in antagonizing oxidative stress in cancer cells. This study was designed to determine how TXNL2 contributes to the regulation of the cellular redox state in cancer cells and redox-mediated signaling pathways. We characterized the molecular actions of TXNL2 and its involvement in tumor development and metastasis and also examined the clinical significance of its expression in primary human breast cancers. Our studies demonstrate that TXNL2 is essential for cancer cell functions by regulating ROS levels and NF-κB activity.

Results

TXNL2 is overexpressed in human cancers. We first compared the expression levels of TXNL2 in normal breast tissues and breast cancer tissues using the Oncomine database, which includes publicly available cDNA microarray data on cancer. Analysis of a representative data set (35) indicated *TXNL2* mRNA levels were higher in breast cancer tissue than in normal breast tissues (Figure 1A). As

Table 1
Statistical analysis of TXNL2 expression in human breast tissues

		TXNL2		
	Case	+ (%)	– (%)	*P* value
Breast cancer	190	114 (60%)	76 (40%)	
Normal tissue	15	1 (7%)	14 (93%)	0.000051

TXNL2-negative expression (staining) and TXNL2-positive expression (staining) are indicated by "–" and "+", respectively.

different cancers commonly possess strong antioxidant capacity to counteract ROS, we also analyzed gene expression profiles of other cancers. *TXNL2* mRNA levels were also elevated in lung cancer (36), colon cancer (ref. 37 and Figure 1A), gastric cancer (38), bladder cancer (39), and cervical cancer (40) (Supplemental Figure 1, A–C; supplemental material available online with this article; doi:10.1172/JCI43144DS1). Thus, increased TXNL2 expression is associated with multiple human cancers.

We then examined TXNL2 expression in human breast cancer cell lines and normal human mammary epithelial cells (HMECs). Immunoblotting showed higher TXNL2 levels in breast cancer cell lines compared with HMECs (Figure 1B). Next, we performed immunohistochemistry of TXNL2 on tissue microarrays containing 190 samples of human invasive breast carcinomas of various subtypes and 15 samples of normal human breast tissues. Tissue staining was scored on the basis of the intensity of TXNL2 labeling and the percentage of TXNL2-positive tumor cells. As illustrated in Figure 1C and Table 1, TXNL2 protein was not detected or was weakly detected in most normal breast tissues but was readily detectable in most invasive breast carcinomas. Normal mouse IgG was used as a negative control (Supplemental Figure 1D). Breast cancer tissues showed significantly higher TXNL2 levels than normal breast tissues ($P < 0.0001$).

TXNL2 knockdown inhibits growth of breast cancer cells. Since TXNL2 levels were consistently higher in breast cancer cell lines, we used shRNA to generate TXNL2-knockdown (TXNL2-KD) cell models to study the function of TXNL2. As shown in Supplemental Figure 2A, 2 TXNL2 shRNAs caused a similar degree of TXNL2 knockdown, without affecting Trx-1 and Grx-1 levels. For simplicity of interpretation, the effects of a representative shRNA are described here. We first explored the effect of TXNL2 downregulation on cell growth using MDA-MB-231 and BT549 human breast cancer cells. Inhibition of TXNL2 suppressed the growth of breast cancer cells but not normal HMECs (Figure 2A), suggesting that TXNL2 is essential for the growth of breast cancer cells. Next, we performed soft agar assays and Matrigel 3D culture. As shown in Figure 2B, depletion of TXNL2 prevented the colony formation of MDA-MB-231 and BT549 cells in soft agar, indicating that anchorage-independent growth was suppressed. Similarly, TXNL2 knockdown disrupted the growth of these cells in Matrigel (Figure 2C). Interestingly, in contrast to that of control cells, which formed stretching-out stellate structures, TXNL2-KD MDA-MB-231 and BT549 cells showed a spherical structure in Matrigel culture (Figure 2C). Similar effects of TXNL2 depletion on growth of 4T1 and MCF-7

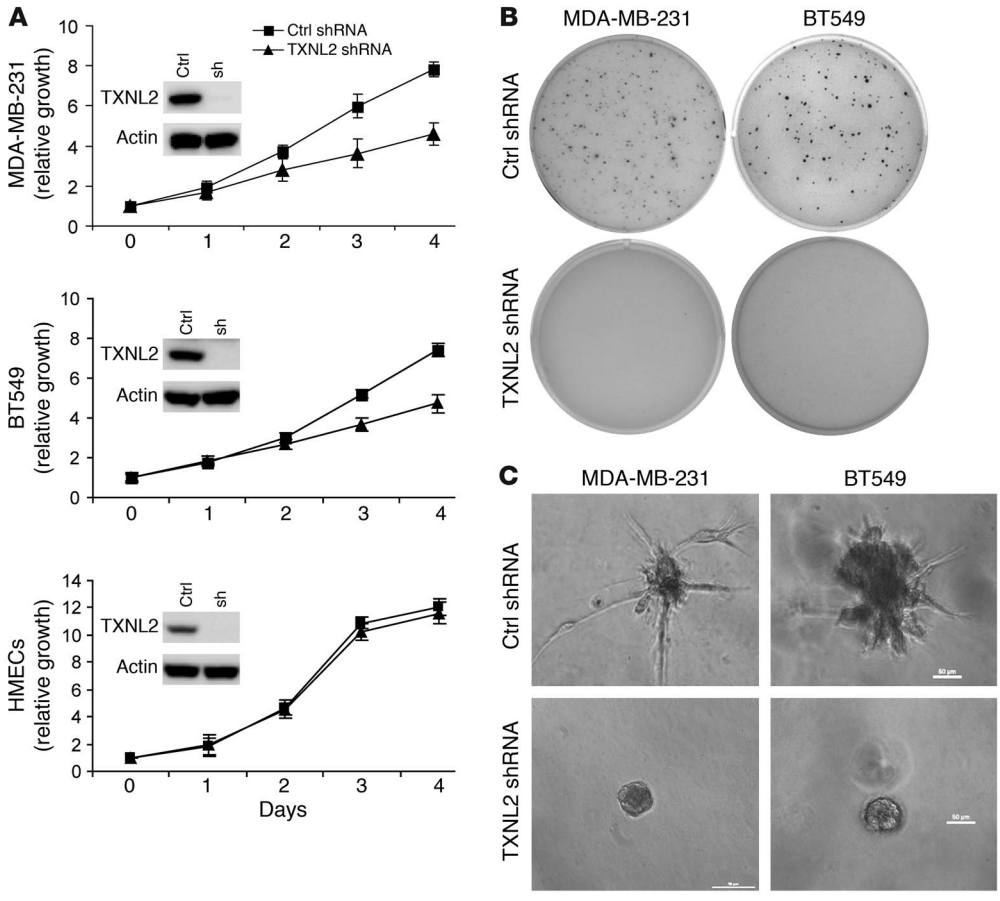

Figure 2
Knockdown of TXNL2 in breast cancer cells inhibits cell growth. (**A**) Cell proliferation was measured using MTT assays, and growth curves of control and TXNL2-KD cells are plotted. The data represent mean ± SD of 3 experiments. The inserts show immunoblots of TXNL2 expression in control (ctrl) and TXNL2-KD (sh) cells. (**B**) Colony formation of control and TXNL2-KD cells in soft agar after 14 days of culture. (**C**) The growth of control and TXNL2-KD cells in 3D Matrigel is shown (original magnification, ×200).

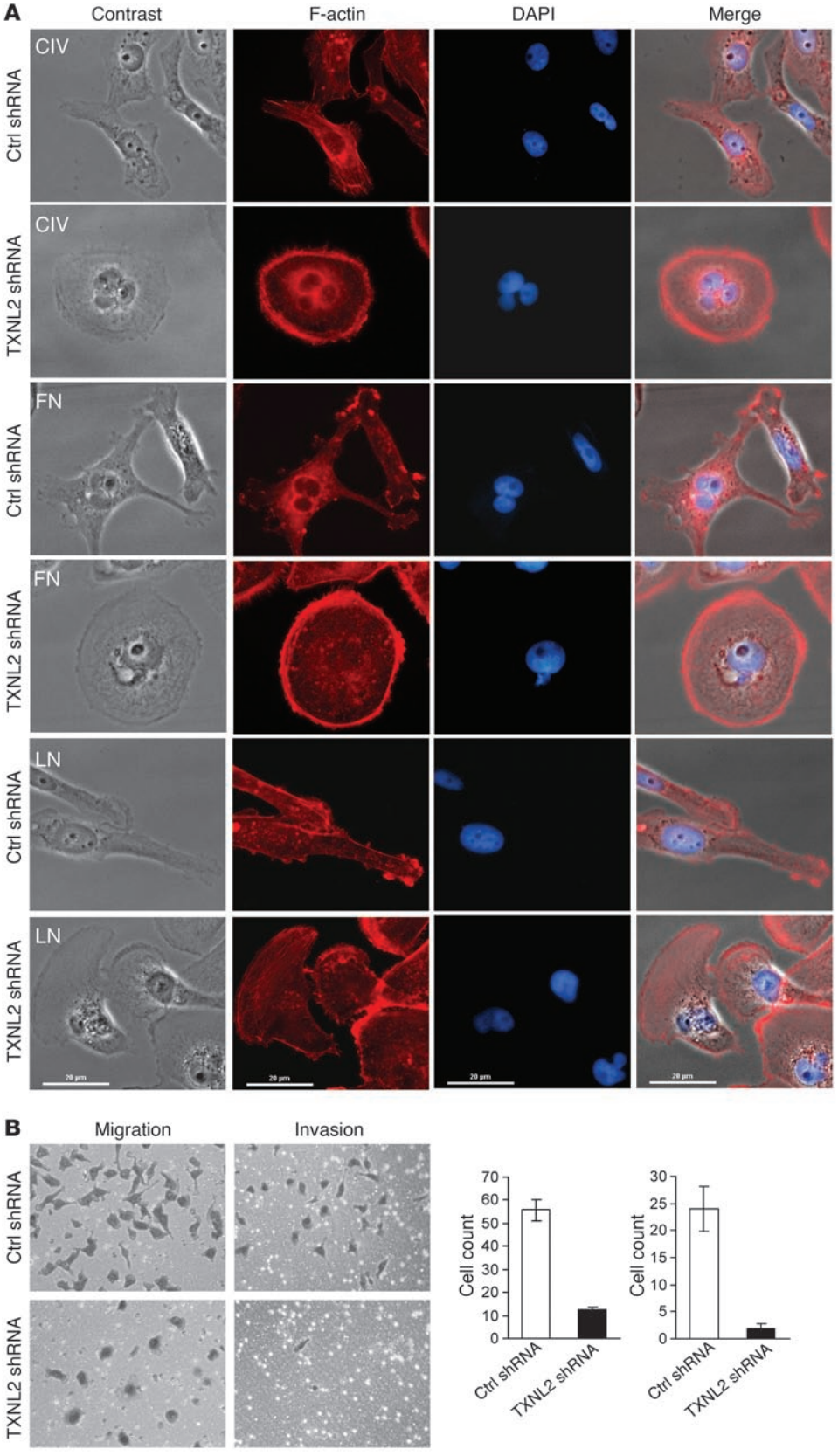

Figure 3
Knockdown of TXNL2 blocks the motility of MDA-MB-231 cells. (**A**) Cell morphologies on different extracellular matrix surfaces are shown. Control and TXNL2-KD MDA-MB-231 cells were plated on collagen IV (CIV), fibronectin (FN), and lamin (LN). F-actin was stained with Alexa Fluor–labeled phalloidin. DAPI was used to visualize cell nuclei (original magnification, ×400). (**B**) Migration and invasion of control and TXNL2-KD cells were measured using transwell chamber assays. Data represent the average cell number from 5 viewing fields (original magnification, ×200).

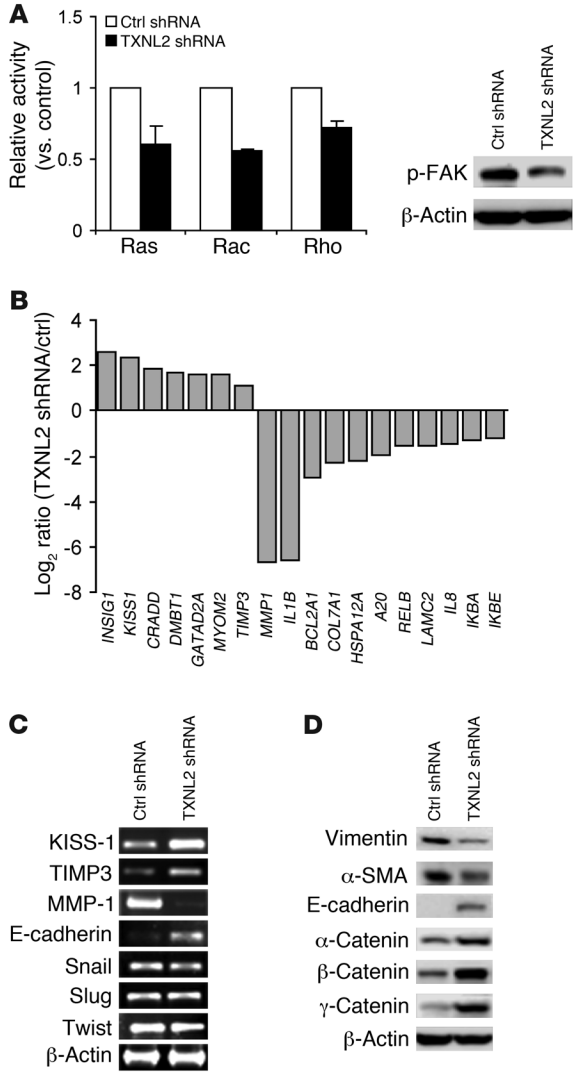

Figure 4
Knockdown of TXNL2 alters small GTPase activity and cell motility-associated gene expression. (**A**) Relative activities of Ras, RhoA, and Rac are plotted. Error bars indicate SD. p-FAK was examined using Western blotting. (**B**) Log_2 ratios of normalized intensity (TXNL2-KD/control) for top-ranked upregulated/downregulated genes in the microarray analysis of TXNL2-KD cells. (**C**) Expression of KISS-1, TIMP3, MMP-1, E-cadherin, Snail, Slug, and Twist was measured using RT-PCR, with β-actin as a control. (**D**) Expression of mesenchymal markers (vimentin and α-SMA) and epithelial markers (E-cadherin and α-, β-, and γ-catenin) was measured using immunoblotting.

breast cancer cells were observed (Supplemental Figure 2, B and C). These results indicate that deficiency of TXNL2 specifically inhibits breast cancer cell growth in monolayer and 3D culture.

TXNL2 knockdown reverses epithelial-mesenchymal transition in breast cancer cells. Notably, knockdown of TXNL2 resulted in a change from mesenchymal-to-epithelial morphology in MDA-MB-231 and BT549 cells (Supplemental Figure 3A). Using immunofluorescence microscopy, we found that TXNL2-KD MDA-MB-231 cells displayed a flattened and cubical morphology, with non-polarized lamellar extensions around the entire cell periphery but no stress fiber formation when plated on different extracellular matrices, such as collagen IV, fibronectin, and laminin (Figure 3A). In contrast, control cells exhibited spindle-like fibroblast morphology, with bundles of stress fibers paralleling the long axis of cells. Similar results were observed in TXNL2-KD BT549 and 4T1 cells (data not shown).

We then explored whether these morphological changes were associated with altered cell motility and invasiveness. To this end, Boyden chamber assays were conducted. TXNL2 knockdown in MDA-MB-231 cells inhibited cell migration and invasion in vitro (Figure 3B). TXNL2-KD cells also showed reduced migration capabilities in wound-healing assays (Supplemental Figure 3B). Furthermore, TXNL2-KD cells at the edges of the wound did not form lamellipodia and moved collectively toward the wound center, as shown by F-actin staining, while control cells displayed polarization toward the wound site and migrated individually (Supplemental Figure 3B). TXNL2 depletion in 4T1 (Supplemental Figure 3, C and D) and BT549 cells (data not shown) also led to impaired migration and invasion.

As small GTPase proteins are well known to be involved in stress fiber formation and cell movement (41), we measured Ras, RhoA, and Rac1 activity in control and TXNL2-KD cells using kinase activity assays. Activation of the focal adhesion kinase (FAK), which relays extracellular matrix signaling, was examined using Western blotting. As expected, activity/activation of Ras, RhoA, Rac1, and FAK was lower in TXNL2-KD cells than in control cells (Figure 4A).

We next compared the transcriptional profiles of control and TXNL2-KD MDA-MB-231 cells using cDNA microarray analysis. As illustrated in Figure 4B, genes with the highest fold changes are involved in cell survival and metastasis. Semiquantitative RT-PCR results corroborated that the invasion/metastasis inhibitors KISS-1 and TIMP3 were upregulated, while the invasion/metastasis promoters MMP-1 (42) and IL-1β (43) were downregulated in TXNL2-KD cells (Figure 4C and Supplemental Table 1). Since TXNL2 knockdown induced a change from a mesenchymal to an epithelial shape, we then measured epithelial-mesenchymal transition (EMT) markers in control and TXNL2-KD cells. Although the expression of EMT transcriptional factors Snail, Slug, and Twist did not change in TXNL2-KD cells (Figure 4C), epithelial markers (E-cadherin and α-, β-, and γ-catenin) were upregulated, while mesenchymal markers (vimentin and α-SMA) were downregulated in TXNL2-KD cells (Figure 4D). Similar results were also observed in BT549 TXNL2-KD cells (Supplemental Figure 3E). In summary, our data suggest that TXNL2 knockdown in breast cancer cells results in reversal of EMT and inhibition of cell migration and invasion.

TXNL2 knockdown induces intracellular ROS accumulation. TXNL2 has Trx-like and Grx domains and can rescue the yeast *grx3/4* mutant under oxidative stress (data not shown). We thus hypothesized that TXNL2 may play an important role in maintaining cell redox homeostasis in response to stress. To address this question, we first measured ROS levels using flow cytometry after dichlorofluorescein diacetate (DCFH-DA) staining in control and TXNL2-KD cells. ROS levels in TXNL2-KD MDA-MB-231 and BT549 cells were higher than those in control cells (Figure 5A). Apoptosis was also increased by TXNL2 depletion, as detected by Annexin V/propidium iodide (Annexin V/PI) staining, followed by flow cytometry (Figure 5A) and cleaved caspase-3 staining (Supplemental Figure 4A). Similar results were found in cells treated with the ROS inducers H_2O_2 and diamide (Figure 5B).

GSH is the most abundant ROS scavenger in mammalian cells, and GSH/GSH disulfide (GSH/GSSG) equilibrium is a major indi-

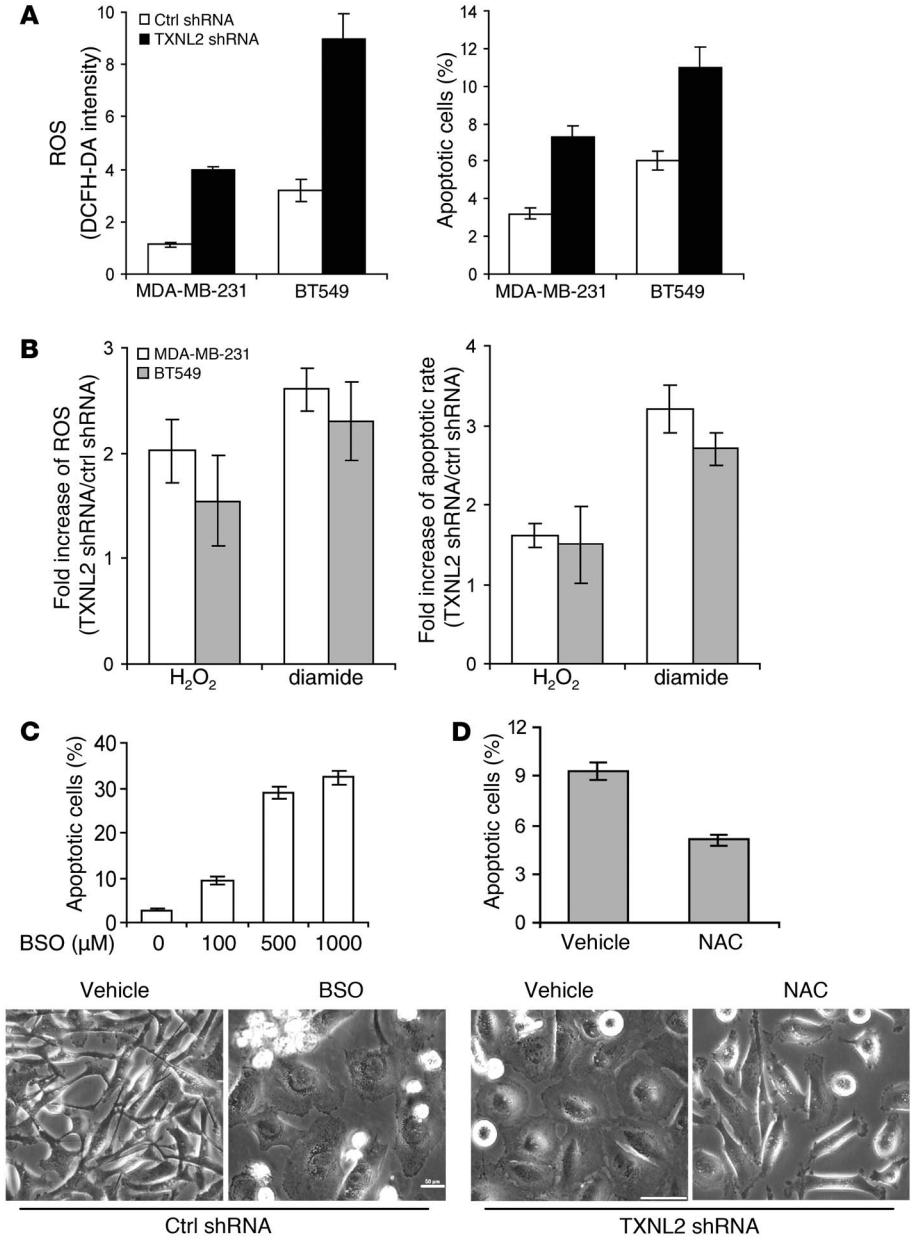

Figure 5
Knockdown of TXNL2 increases intracellular ROS. (**A**) ROS levels were measured using DCFH-DA staining, followed by flow cytometry. Cell apoptosis was measured using Annexin V/PI double staining, followed by flow cytometry. (**B**) Intracellular ROS and cell apoptosis were measured in control and TXNL2-KD cells after treatment with H_2O_2 or diamide. Fold increases of ROS and apoptotic rate (TXNL2-KD/control) are plotted. (**C**) BSO-induced apoptosis in control MDA-MB-231 cells was measured using Annexin V/PI staining, and apoptotic rates are plotted. Images show cell morphologies without and with BSO treatment. (**D**) Cell apoptosis was measured using Annexin V/PI staining in TXNL2-KD MDA-MB-231 cells treated with or without NAC for 48 hours. Morphologies of TXNL2-KD cells treated with or without NAC are shown. Scale bar: 50 μm.

cator for oxidative stress (44). The GSH/GSSG ratio, commonly used to define oxidative stress in culture cells (45), was markedly lowered in TXNL2-KD cells (Supplemental Figure 4B). The GSH biosynthesis inhibitor buthionine sulfoximine (BSO), like TXNL2 shRNA, increased cell apoptosis and elicited an epithelial shape in MDA-MB-231 cells (Figure 5C). In contrast, *N*-acetyl-cysteine (NAC, a metabolic precursor of GSH) (46) partially inhibited apoptosis and restored fibroblast morphology in TXNL2-KD cells (Figure 5D). The same effects were shown in control and TXNL2-KD BT549 cells (Supplemental Figure 4C) treated with BSO and NAC. Taken together, these results suggest that TXNL2 modulates intracellular oxidative stress in cancer cells.

Both Trx-1 and Grx-1 are well-known ROS scavengers and involved in cellular redox regulation (30). PX-12, a small-molecule inhibitor of Trx-1 (24), did not inhibit growth or increase ROS levels in MDA-MB-231 cells, although it had a moderate effect on MCF-7 cells (Supplemental Figure 4, D and E). These results suggest that the effects of TXNL2 depletion were not primarily mediated by Trx-1 or Grx-1 inhibition. Of note, TXNL2 knockdown did not induce a significant increase of ROS levels in HMECs (data not shown), which may explain why TXNL2 knockdown did not affect the growth of HMECs.

TXNL2 knockdown inhibits NF-κB activity. Because the expression of NF-κB–regulated genes such as *RELB*, *IL1B*, *IL8*, *BCL2A1*, *A20*, and *IKBA* (47–49) was altered in TXNL2-KD cells (Figure 6A) and because NF-κB is regulated by ROS (50), we speculated that NF-κB activity might be downregulated by TXNL2 depletion. Thus, we examined NF-κB components by Western blotting. As illustrated in Figure 6B, levels of total RelB and phosphorylated p65 (p-p65; Ser536) were reduced by TXNL2 knockdown, implicating lower NF-κB activity. Immunofluorescence staining also showed less p65 nuclear localization in TXNL2-KD cells (Figure 6C and Supplemental Figure 5A),

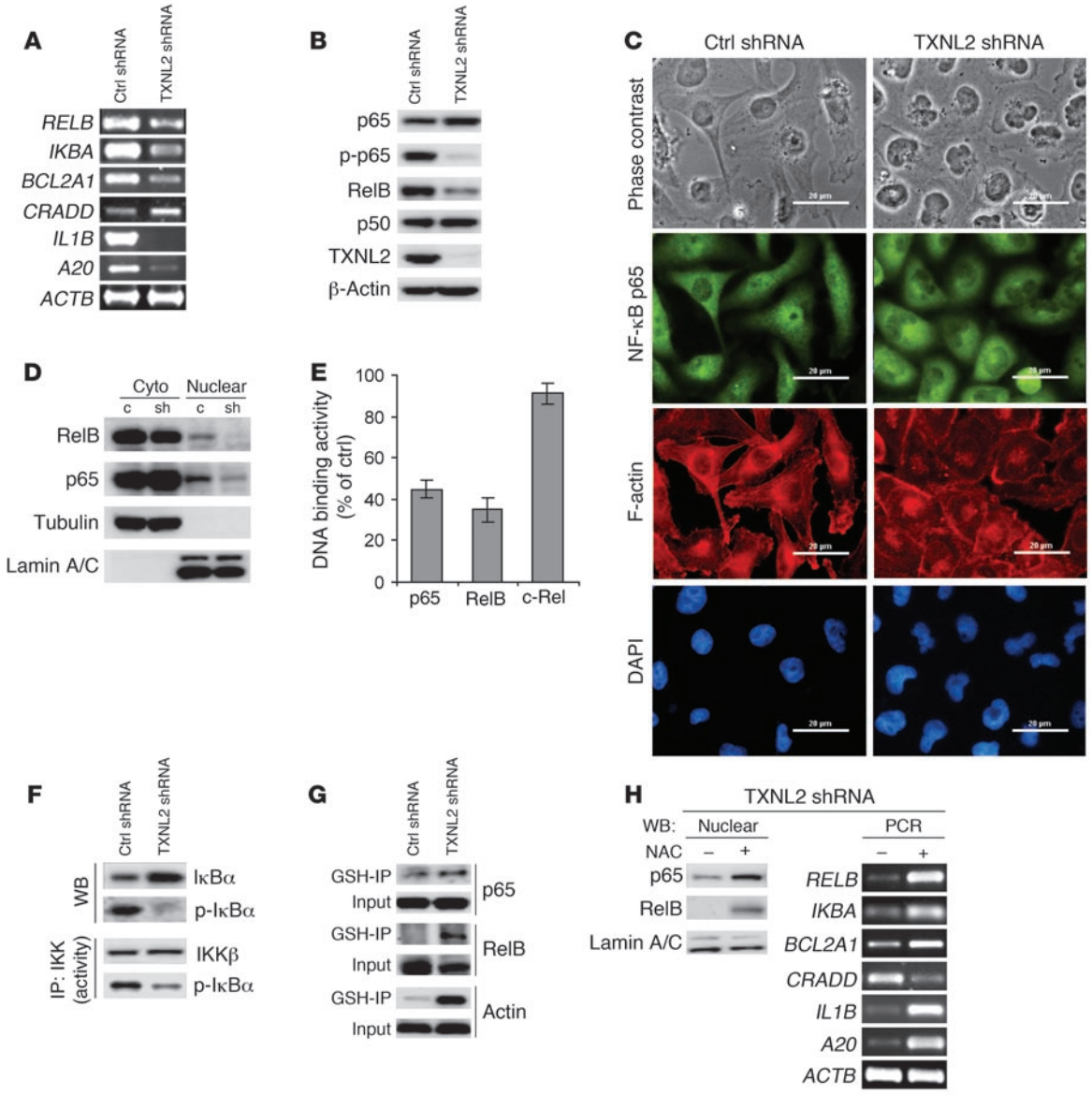

Figure 6

TXNL2 knockdown blocks NF-κB activity in breast cancer cells. (**A**) Expression of NF-κB–regulated genes in control and TXNL2-KD cells was measured using semiquantitative RT-PCR. (**B**) Expression of NF-κB components was examined using immunoblotting. (**C**) Nuclear localization of p65 in control and TXNL2-KD MDA-MB-231 cells was visualized using indirect immunofluorescence staining. F-actin (red) was used to show cell morphology, and DAPI (blue) was used to show nuclei. Scale bar: 20 μm. (**D**) Expression of p65 and RelB in cytosolic (cyto) and nuclear fractions from control (c) and TXNL2 shRNA (sh) cells was examined using immunoblotting. Tubulin and lamin A/C were used as cytoplasmic and nuclear markers, respectively. (**E**) The relative DNA binding activities (% of control) of p65, RelB, and c-Rel were measured by TransAM DNA-binding ELISA. Data represent mean ± SD of 3 experiments. (**F**) In vitro IKK activity assays were performed. IKK activity was indicated by p-IκBα levels. Total IκBα and p-IκBα levels in control and TXNL2-KD cells were assessed using immunoblotting. (**G**) Glutathionylation of p65 and RelB was examined using GSH immunoprecipitation, followed by immunoblotting. (**H**) TXNL2-KD MDA-MB-231 cells were treated with NAC for 6 hours. Nuclear localization of p65 and RelB was examined by immunoblotting. NF-κB–regulated genes were measured by semiquantitative RT-PCR.

which was confirmed by immunoblotting with nuclear and cytosolic extracts (Figure 6D). Using the TransAM DNA-binding ELISA, we found that p65 and RelB DNA binding activity was suppressed in TXNL2-KD MDA-MB-231 and BT549 cells, while c-Rel activity was unaltered (Figure 6E and Supplemental Figure 5, A and B). These results suggest TXNL2 depletion inhibits NF-κB activity. To determine the clinical relevance of this association between TXNL2 and p65, we further examined the nuclear localization of p65, which has been used to recognize the active state of NF-κB (51, 52). In 190 human breast cancer specimens, immunohistochemical analysis demonstrated that TXNL2 positivity was significantly associated with the nuclear expression of p65 (Table 2).

In line with the inactivation of p65 by TXNL2 deficiency, immunoblotting showed that levels of IκBα, an NF-κB inhibitor caus-

Table 2
Association between TXNL2 expression and p65 nuclear staining examined by immunohistochemistry in 190 human breast cancer specimens

	TXNL2 (+)	TXNL2 (–)	*P* value
Nuclear p65 (+)	83	24	
Nuclear p65 (–)	31	52	< 0.0001

Association was examined using the χ^2 test. The cutoff score for TXNL2 is the same as in Table 1.

ing p65 cytoplasmic retention, were increased, whereas IκBα phosphorylation at Ser32 (a key signal for IκBα degradation) was decreased in TXNL2-KD MDA-MB-231 cells (Figure 6F). This suggests stabilization of IκBα protein. IKK activity is reportedly inhibited by oxidative stress (53). Not surprisingly, lower IKK activity was found in TXNL2-KD cells (Figure 6F), as shown by less IκBα phosphorylation in IKK kinase assays (54, 55). Although AP-1 transcriptional factors can also be regulated by redox state (56), their activity was not consistently and significantly inhibited in TXNL2-KD cells (data not shown).

Given that high levels of GSSG can convert the NF-κB heterodimers into an oxidized form with little or no DNA binding activity (57) and that TXNL2-KD cells contain low GSH/GSSG ratio, we investigated whether NF-κB was oxidized in these cells. GSH immunoprecipitation followed by immunoblotting indicated increased glutathionylation of p65 and RelB (Figure 6G), which would decrease their activity. Of note, actin displayed increased glutathionylation in TXNL2-KD cells, as indicated by the increased amount of immunoprecipitated actin by GSH antibody. In line with these results, the nuclear localization of p65 and RelB as well as the expression of NF-κB–regulated genes (see Figure 6A) in TXNL2-KD cells was rescued by NAC treatment (Figure 6H and Supplemental Figure 5C).

To further rule out potential off-target effects of shRNA, we suppressed TXNL2 expression by siRNA that had TXNL2-targeting sequences distinct from those of shRNA (see Methods and Supplemental Table 2). As expected, NF-κB activity decreased and ROS levels increased (Supplementary Figure 5D). Furthermore, ectopic expression of the mouse *Txnl2* gene in TXNL2-KD MDA-MB-231 cells restored levels of nuclear p65, p-p65, IκBα, and EMT markers and reversed fibroblast morphology (Supplemental Figure 5E). Collectively, these observations demonstrate that TXNL2 depletion inhibits NF-κB activity by increasing ROS levels.

NF-κB mediates the effect of TXNL2 knockdown on mesenchymal-epithelial transition. Because NF-κB regulates cell functions, including EMT (58), we asked whether NF-κB mediates the effects of TXNL2 knockdown. When the IKK inhibitor BMS-345541 was used to block NF-κB activity in MDA-MD-231 and BT549 cells, the fibroblast morphology changed to a cuboidal shape (Figure 7A) and was accompanied by changes in the expression of NF-κB–regulated genes (Figure 7B). These BMS-induced phenotypes were reminiscent of those in TXNL2-KD cells. Similar results were found in MDA-MB-231 cells treated by other NF-κB inhibitors, such as BAY-117082 and JSH-23 (data not shown). As expected, pharmacologic inhibition of NF-κB inhibited cell growth, migration, and invasion (Supplemental Figure 6A).

We next examined Akt activation by immunoblotting p-Akt, since Akt is reportedly involved in the stress response (59). Akt activation was lower in TXNL2-KD MDA-MB-231 (Figure 7C) and BT549 (Supplemental Figure 6B) cells. Blocking Akt activity using Akt inhibitor IV (AI-IV), unlike NF-κB blockade, did not induce mesenchymal-epithelial transition (MET) in both cell lines (Supplemental Figure 6C) but elicited apoptosis and growth inhibition (Figure 7D). This suggests that Akt may be involved in mediating the effect of TXNL2 on cell survival but not the EMT process in breast cancer cells.

Akt can be downstream (60) or upstream of NF-κB (61). To address this, we generated IκBα S32A/S36A super-repressor–overexpressing (IκBα-SR-overexpressing) MDA-MD-231 cells. As shown in Figure 7E, p-Akt was downregulated in these cells, which also displayed MET. In agreement with this, p65 nuclear localization and p-Akt were markedly reduced by the IKK inhibitor BMS. In contrast, p65 nuclear localization was not blocked by AI-IV (Figure 7F). To further investigate the mechanism of p65 in TXNL2-regulated signaling, we overexpressed p65 in TXNL2-KD MDA-MB-231 cells. RelB expression, which is a known target of p65, was dramatically increased, whereas TXNL2 expression was not upregulated by NF-κB (Supplemental Figure 6D). Notably, the p-Akt level was induced by p65 overexpression, further indicating that NF-κB mediates the effect of TXNL2 on Akt activation. Fibroblast morphology and invasion ability were also restored in p65-overexpressing TXNL2-KD MDA-MB-231 cells. Together with our findings that Snail, Slug, and Twist were not inhibited by TXNL2 depletion, these data suggest that NF-κB mediates the effects of TXNL2 on breast cancer cells and that Akt acts downstream of NF-κB to regulate cell survival and proliferation (Figure 7G).

TXNL2 is critical for tumorigenesis and metastasis in vivo. We next tested whether TXNL2 knockdown inhibits tumor growth in vivo. Control and TXNL2-KD MDA-MB-231 cells were injected orthotopically into the mammary fat pads of SCID mice and tumor growth was examined. Mice injected with control cells formed large tumors within 37 days, whereas mice injected with TXNL2-KD cells showed greatly reduced tumor growth (Figure 8A). These results indicate that TXNL2 expression is necessary for optimal growth of breast cancer cells in the mammary fat pads of mice. Because MDA-MB-231 cells have a high metastatic potential in vivo (62), we examined the lungs from mice with control and TXNL2-KD mammary tumors. As shown in Figure 8B, TXNL2 depletion substantially suppressed the formation of lung metastases after injection of MDA-MB-231 cells in the mammary fat pads.

Because the reduced lung metastasis might be due to slower primary tumor growth, we further evaluated the in vivo effects of TXNL2 on breast cancer lung metastasis, using an experimental metastasis assay. Control or TXNL2-KD cells were injected into the lateral tail veins of SCID mice. After 4 weeks, the average number of metastatic nodules per lung was 120 in mice injected with control cells but only 30 in mice injected with TXNL2-KD cells (Figure 8C). The lungs from control mice were not extensively stained by black India ink, a commonly used method to visualize pulmonary macrometastases, as the lung tissue was replaced by tumor cells. In contrast, the lungs from mice injected with TXNL2-KD cells were stained by the dye. Our data indicate that TXNL2 controls the highly metastatic behavior of MDA-MB-231 cells.

TXNL2 overexpression predicts distant metastasis of human breast cancer to the lung and brain. Given the above results, we further examined the clinical significance of TXNL2 overexpression in primary human breast cancer, using gene expression microarray analysis of a 192-sample data set with known metastasis profiles (63). Elevat-

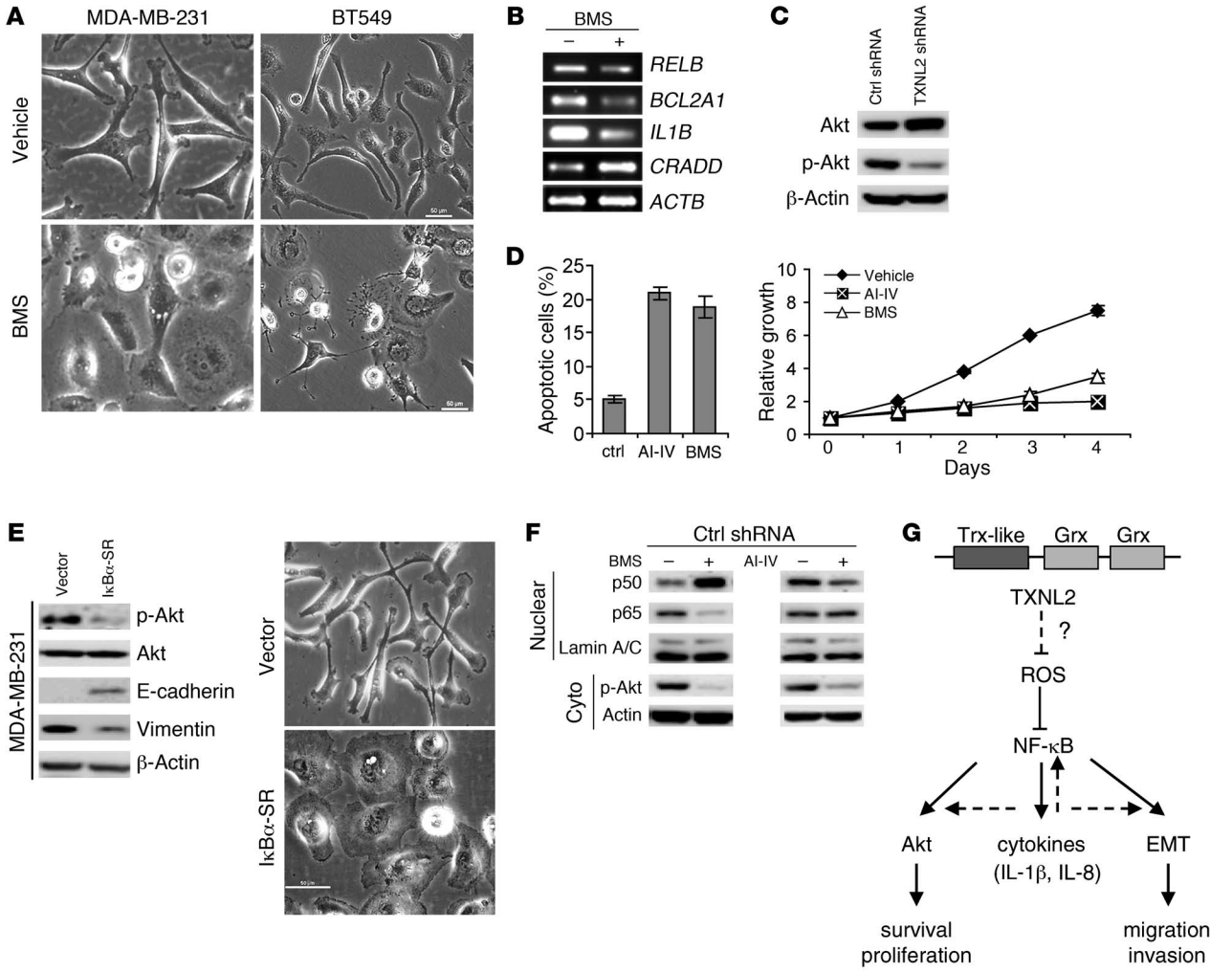

Figure 7

NF-κB is essential for the effects of TXNL2 on cell survival and EMT. (**A**) Morphologies of control MDA-MB-231 and BT549 cells treated with the IKK inhibitor BMS-345541 (BMS) or DMSO for 24 hours are shown (original magnification, ×200). (**B**) Expression of NF-κB–regulated genes was measured using RT-PCR in MDA-MB-231 cells treated with BMS-345541 or DMSO. (**C**) Total Akt and p-Akt levels in control and TXNL2-KD MDA-MB-231 cells were measured using Western blotting. (**D**) Apoptosis was measured using Annexin V/PI staining in MDA-MB-231 cells treated with vehicle (ctrl), AI-IV, or BMS. Data represent mean ± SD of 3 independent experiments. Growth curves of cells treated with or without inhibitors are plotted. (**E**) Akt activation and EMT markers (E-cadherin and vimentin) in IκBα-SR–overexpressing and control MDA-MB-231 cells were measured using Western blotting. Cell morphologies are shown (original magnification, ×200). (**F**) The expression of NF-κB and Akt after BMS or AI-IV treatment was examined using Western blotting. (**G**) A schematic diagram of TXNL2 signaling. Broken lines indicate pathways, based on previous reports. The question mark denotes currently unknown mechanisms.

ed TXNL2 expression was positively associated with lung metastasis ($P = 0.0097$) and brain metastasis ($P = 0.0267$) and significantly correlated with shorter lung metastasis-free survival ($P < 0.0001$; Figure 9A) and brain metastasis-free survival ($P < 0.011$; Figure 9B). This statistically significant association was consistently observed at multiple arbitrary percentile cutoff points (25th, 50th, 75th, and 90th) used for purposes of creating dichotomous groups to facilitate data analysis. The risk of developing lung metastasis was 44.1% for each unit increase relative to the *TXNL2* mRNA level (hazard ratio 1.441, 95% CI, 1.217–1.707). Thus, TXNL2 may serve as a prognostic marker for breast cancer metastasis. Analysis of 2 additional data sets (64, 65) lent further support to the clinical impact of enhanced *TXNL2* mRNA expression. Elevated TXNL2 expression was found to correlate with decreased recurrence-free survival ($P < 0.003$; Figure 10A), decreased distant-metastasis free survival ($P < 0.012$; Figure 10A), decreased disease-specific survival ($P < 0.005$; Figure 10B), and decreased overall survival ($P < 0.030$; Figure 10B). Thus, TXNL2 may serve as a prognostic marker for breast cancer metastasis and survival.

Discussion

Although increased TXNL2 expression in various solid tumors has been reported in another study (66), our study is the first to our knowledge to investigate TXNL2 function in cancer cells. We found that TXNL2 knockdown increased intracellular ROS levels and decreased the GSH/GSSG ratio, thereby inhibiting cell growth, survival, and invasion. These TXNL2 effects were mediated by NF-κB signaling (see Figure 7G). Xenograft models showed that

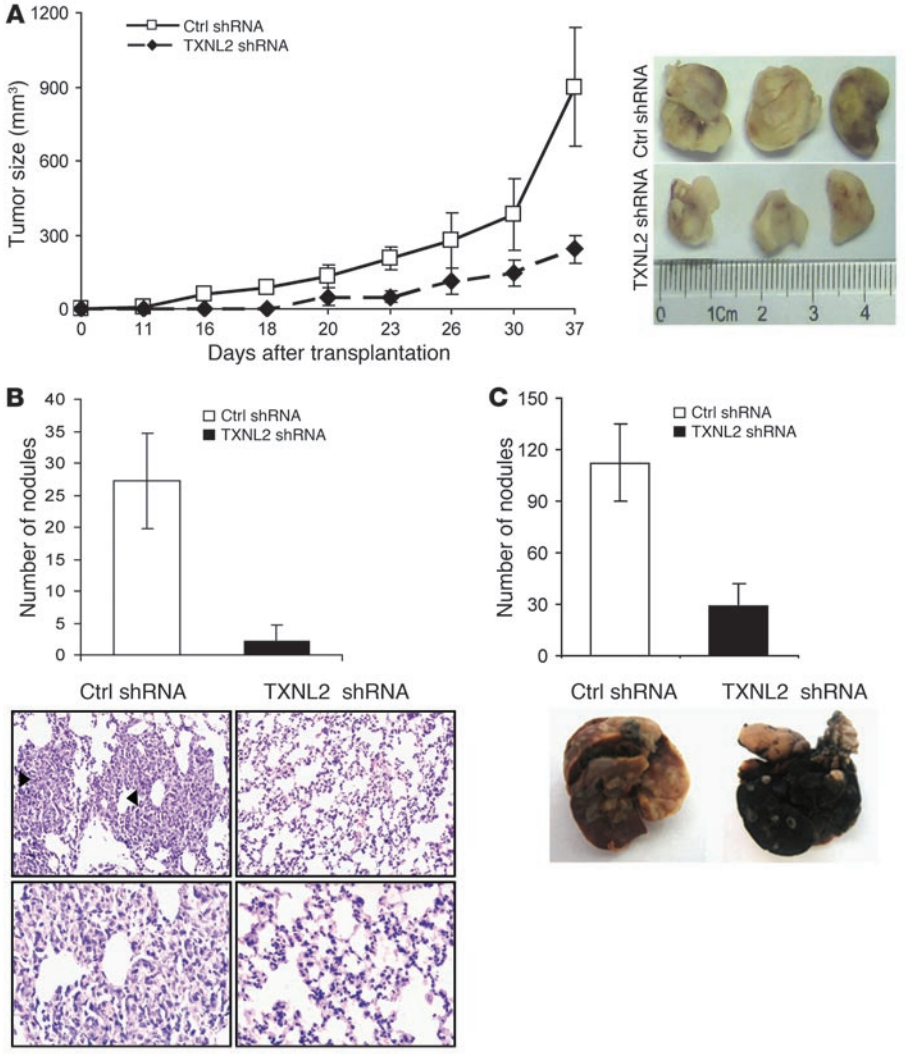

Figure 8
TXNL2 knockdown inhibits tumorigenic and metastatic capabilities of MDA-MB-231 cells. (**A**) Growth curves of mammary tumors after orthotopic injection of control and TXNL2-KD MDA-MB-231 cells in SCID mice. Data represent mean ± SD (n = 10). (**B**) Number of metastatic nodules per lung after injection of control and TXNL2-KD MDA-MB-231 cells in mouse fat pads (n = 10). Representative micrographs of lung tissues with metastatic cells (arrowheads) are shown. Original magnification, ×200 (top); ×400 (bottom). (**C**) The number of metastatic nodules per lung in control and TXNL2-KD groups 40 days after tail vein injections is plotted as mean ± SD (n = 10). Representative pictures of lungs stained by India ink are shown.

TXNL2 deficiency inhibited tumor growth and lung metastasis. The correlation between elevated TXNL2 expression and metastasis to the lung or brain was demonstrated using gene expression microarray analysis. Our data suggest that TXNL2 may be a critical factor for redox homeostasis and breast cancer tumorigenesis and metastasis and may serve as a therapeutic target.

TXNL2 is a key component in regulating intracellular ROS levels. Cancer cells generate higher ROS levels, partially due to a higher metabolic rate, but cancer cells have strong ROS scavenging systems (67). Upsetting this balance by further increasing ROS generation or inhibiting antioxidative capacity can cause cell death. As mentioned above, TXNL2 is consistently overexpressed in many breast cancer cell lines. Further increasing its levels in noninvasive MCF-7 cells only mildly enhanced cell growth and invasion (our unpublished observations). We postulate that TXNL2 is essential but may not be sufficient to induce aggressive behavior associated with tumor cells.

TXNL2, although lacking the conserved Cys-Gly-Pro-Cys Trx motif that is essential for catalytic activity (29), may be able to modulate ROS levels via its Grx domains. A recent structural analysis of the TXNL2 yeast homolog confirmed that the cysteine in Grx domain may have catalytic activity (68). This is also supported by a recent study, indicating that TXNL2 binds 2 bridging [2Fe-2S] clusters in a homodimeric complex with the active site Cys residues of its 2 Grx domains and GSH bound non-covalently to the Grx domains (69).

Recent studies indicate that TXNL2 is able to protect yeast cells against oxidative stress and that TXNL2 deficiency causes embryonic lethality (34) (our unpublished observations). By using a yeast 2-hybrid technique, we identified several TXNL2-interacting proteins, including oxidation-regulating proteins such as metallothionein 2A, malate dehydrogenase 1, and cystatin C (our unpublished observations). These results implicate TXNL2 in cellular responses to stress signals, particularly ROS. Mechanically, how TXNL2 controls ROS levels is not understood. The increase of ROS by TXNL2 depletion may lead to a lower GSH/GSSG ratio. Alternatively, TXNL2 may regulate ROS levels through first modulating the GSH/GSSG pool. Both scenarios can be supported by our findings that the GSH precursor NAC restored TXNL2-impaired cell functions, while the GSH synthesis inhibitor BSO mimicked the effect of TXNL2 knockdown.

NF-κB mediates the effects of TXNL2 knockdown. Constitutive NF-κB DNA binding activity has been reported in 65% of primary breast cancers (70, 71) and is also associated with other malignancies (72).

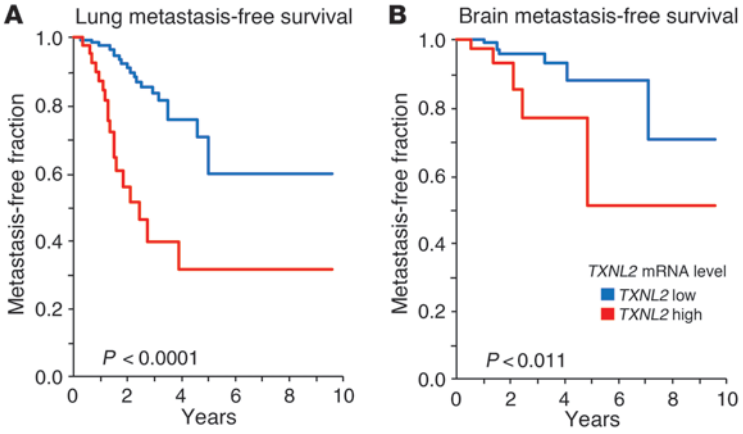

Figure 9
TXNL2 expression in human primary breast cancer predicts the occurrence of metastasis to lung and brain. (**A**) Kaplan-Meier curves of lung metastasis-free survival of breast cancer patients, stratified by *TXNL2* mRNA levels in an 192-sample data set (63). (**B**) Kaplan-Meier plots of brain metastasis-free survival of breast cancer patients, stratified by *TXNL2* mRNA expression from the same data set.

Our studies showed that TXNL2-KD unregulated proapoptotic genes, such as *CRADD* (73), downregulated antiapoptotic genes, such as *BCL2A1* (74), and indirectly decreased Akt activity via reduced NF-κB activity. These results further support that NF-κB plays a central role in mediating the effects of TXNL2 on cell survival.

Notably, *MMP1* emerges as a strongly downregulated gene, while *KISS1* is a strongly upregulated gene in TXNL2-KD cells. MMP-1 is reportedly induced by NF-κB (48, 75) and is a potential prognostic marker of breast cancer (76). Recently, MMP-1 was found to promote breast cancer cell metastasis to bone (42, 62, 77) and lung (78). Consistent with this notion, our experimental metastasis assays showed that TXNL2 knockdown inhibited lung metastasis. KISS-1 is a well-established cancer metastasis inhibitor (79). The MET process, which is also associated with less aggressive cancer cell activity, is induced by inhibition of NF-κB, as shown in our and other studies (58, 80). In addition to the classical NF-κB pathway, RelB also inhibits breast cancer cell apoptosis and maintains the invasive phenotype and mesenchymal characteristics (81). Thus, suppression of RelB activity may also be involved in TXNL2 knockdown-induced effects.

TXNL2 regulates NF-κB activity. One critical regulator of NF-κB is the IKKα/IKKβ/IKKγ complex, which phosphorylates IκBα and thereby releases NF-κB. Our data showed that IKK activity was significantly downregulated in TXNL2-KD cells, consistent with the previous finding that IKKβ activity is regulated by redox state (53). Interestingly, the DNA binding activity and expression level of RelB were suppressed in TXNL2-KD cells. This may be due to reduced NF-κB activity, which controls RelB transcription (48), and reduced IKK activity (82), which governs RelB activation. This mechanism might explain why TXNL2 knockdown has a dramatic effect on NF-κB.

A high ratio of GSH/GSSG provides cells with a reducing environment and maintains proteins in a reduced state. An oxidative environment with high GSSG can promote protein-SSG formation (83). NF-κB activity can be suppressed by oxidation (84). A decrease in the GSH/GSSG ratio may create a more oxidative environment, which subsequently oxidizes NF-κB and diminishes its DNA binding activity (85). S-glutathionylation of the cysteine residues close

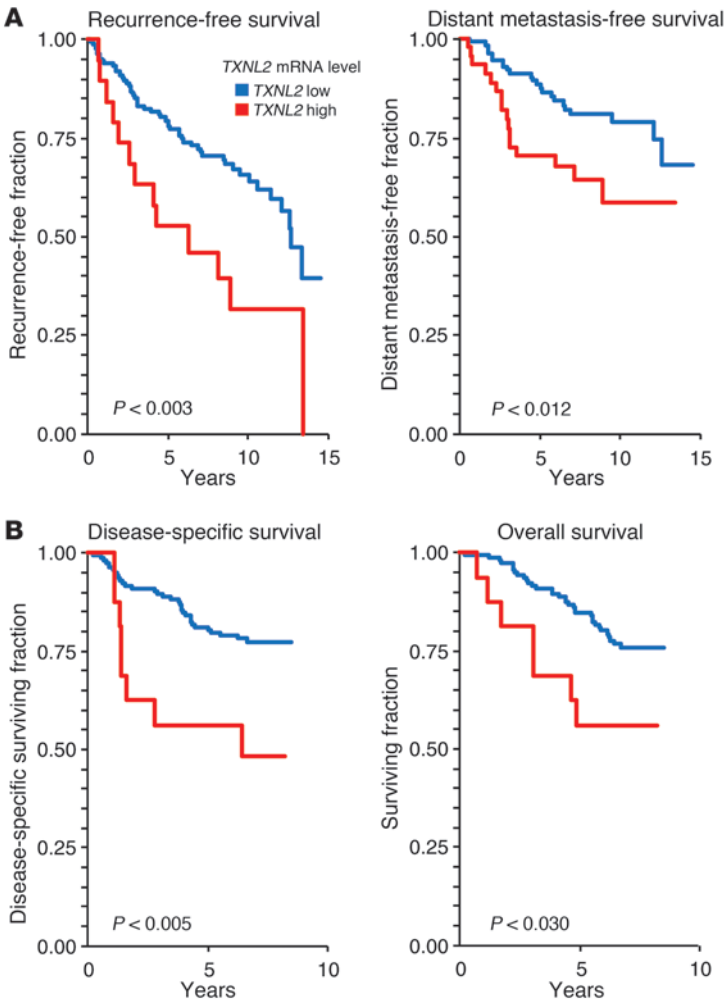

Figure 10
Prognostic significance of TXNL2 in human breast cancer. (**A**) Kaplan-Meier curves of recurrence-free survival and distant metastasis-free survival of breast cancer patients, stratified by *TXNL2* mRNA levels in an 189-sample data set (65). (**B**) Kaplan-Meier curves of disease-specific survival and overall survival of breast cancer patients, stratified by *TXNL2* mRNA levels in an 159-sample data set (64).

to the DNA-binding loops inhibits p65 DNA binding activity (86, 87). A redox balance is required for optimal activation of NF-κB (88). It is known that ROS can activate transcription factors, including NF-κB (85). However, ROS accumulation beyond threshold levels can also inhibit NF-κB activity (89–91). We recently also showed that elesclomol, a novel small-molecule oxidative stress inducer, dramatically suppressed NF-κB activity in breast cancer cells by increasing ROS (92). We found that TXNL2 depletion increased ROS and oxidation of p65 and RelB (indicated by their glutathionylation) and inhibited NF-κB. This effect is similar to the effects of ROS inducers BSO, H_2O_2, and diamide and can be reversed by NAC. Although glutathionylation is reversible, an oxidizing environment due to low GSH/GSSG ratio in TXNL2-KD cells may prevent protein-SSG reduction and thus suppress NF-κB activity.

Additionally, IL-1β and IL-8 are inhibited in TXNL2-KD cells. Thus, feedback regulatory loops between cytokines and NF-κB may also play a role in regulation of NF-κB activity (93–95). Taken together, our results suggest that the regulation of NF-κB by TXNL2 may involve multiple mechanisms.

In summary, the data presented here demonstrate what we believe to be a novel and important role of TXNL2 in regulating cancer cell growth and metastasis through a redox signaling mechanism. The findings that TXNL2 depletion preferentially impacts cancer cells but does not affect normal mammary epithelial cells and that TXNL2 is a critical regulator of NF-κB in cancer cells may have significant clinical implications. Further investigation is warranted to determine whether targeting TXNL2 may be an effective approach to induce ROS in cancer cells.

Methods

Details regarding cell culture, immunofluorescence staining, in vitro migration/invasion, Western blotting, kinase assays, and RT-PCR are provided in the Supplemental Methods.

Immunohistochemistry. Immunohistochemistry was performed by using a highly sensitive streptavidin-biotin-peroxidase detection system with breast cancer tissue microarrays and an in-house generated TXNL2 monoclonal antibody (1:200 dilution). Immunohistochemistry of p65 was conducted using a monoclonal anti-p65 antibody (Santa Cruz Biotechnology Inc.). Positive or negative nuclear staining of p65 was assessed. The tissue microarray slide included 190 cases of breast tumors and 15 cases of normal breast tissues, with duplicate cores for each case (Shanghai Biochip Co.). Methyl green was used as a counterstain. The slides were evaluated microscopically, and the signal was scored using the Allred scoring system (96). The χ^2 test was used to determine the association of TXNL2 staining with normal and tumor tissues.

shRNA and stable transfectants. shRNA constructs in pLKO.1-puro specifically targeting human and mouse TXNL2 sequences were purchased from Sigma-Aldrich. The human TXNL2 shRNA1 sequence is 5′-CCGGGAACGAAGTTATGGCAGAGTTCTCGAGAACTCTGCCATAACTTCGTTCTTTTTG-3′. The human TXNL2 shRNA2 sequence is 5′-CCGGGCTCTTTATGAAAGGAAACAACTCGAGTTGTTTCCTTTCATAAAGAGCTTTTTG-3′. The mouse TXNL2 shRNA1 sequence is 5′-CCGGCCGAAGCTGTTCCTGAAGTATCTCGAGATACTTCAGGAACAGCTTCGGTTTTTG-3′. The mouse TXNL2 shRNA2 is 5′-CCGGGCTAAAGAACACCCTCATGTTCTCGAGAACATGAGGGTGTTCTTTAGCTTTTTG-3′. Control cells were transfected with a control shRNA that does not match any known human or mouse coding cDNA. Stable knockdown clones were pooled and used for experiments.

Microarray data analysis. Gene expression analysis of MDA-MB-231 cells and TXNL2-KD cells was performed using the Human OneArray (Phalanx Biotech Group). Detailed methods are described in the Supplemental Methods. The $\log_2$-transformed expression ratio (TXNL2 shRNA clones versus control clones) of each gene was calculated.

Measurement of ROS production. ROS generation was measured with DCFH-DA (Invitrogen). Cells were incubated with 5 μM DCFH-DA for 30 minutes, followed by flow cytometry using a FACSCalibur (BD Biosciences). The data were analyzed using Cell Quest software (BD Biosciences).

Flow cytometry analysis. ROS generation was measured using DCFH-DA (Invitrogen) staining. Apoptotic cells were analyzed by flow cytometry using Annexin V–FITC and PI staining (BD Biosciences). FACSCalibur was used for flow cytometry, and the data were analyzed using Cell Quest software.

Transient expression reporter gene assay. The NF-κB–responsive luciferase reporter construct in pGL4 was from Promega. The construct was cotransfected with the TXNL2 vector or the control vector. After 24 hours of incubation, the luciferase activity was measured and normalized by β-galactosidase activity (Promega). The data presented are the mean value of 3 independent experiments.

NF-κB transcription factor DNA-binding ELISA assay. The transcription factor NF-κB family activation assay was measured using the TransAM NF-κB Family Kit (Active Motif), according to the manufacturer's instructions.

In vivo tumorigenesis and metastasis. All animal experiments were performed with the approval of Baylor College of Medicine and Tianjin Medical University animal care and use committees. Details are provided in the Supplemental Methods.

Survival analysis. The expression of TXNL2 and its association with metastasis to the lung or brain were examined in breast cancer patients in a 192-patient data set (63). The Wilcoxon rank-sum test was used to assess statistical significance for this comparison. Brain-specific and bone-specific metastasis-free survival was also examined in this data set using the log-rank test, and survival plots were created using Kaplan-Meier methods. The prognostic significance of TXNL2 in predicting recurrence-free survival and distant metastasis-free survival in breast cancer patients was examined in the 189-sample (65) microarray data set. The prognostic significance of TXNL2 in predicting disease-specific survival and overall survival in breast cancer patients was examined in the 159-sample (64) microarray data set. Details regarding the gene expression microarray analysis for the above data sets are provided in the Supplemental Methods.

Statistics. Values represented mean ± SD of samples measured in triplicate. Each experiment was repeated 3 times, unless otherwise indicated. The significance of differences between experimental groups was analyzed using the Student's *t* test and 2-tailed distribution. The χ^2 test was performed to determine the association between TXNL2 levels and p65 nuclear staining in human breast cancer samples.

Acknowledgments

We thank Dave Hoon and Myles Cabot for technical help. We thank Oncothyreon Inc. for providing PX-12. We thank Gwen Berry and Yukun Cui for helpful suggestions and critical reading of the manuscript. This work was supported by Susan G. Komen Breast Cancer Foundation (BCTR0601346 to X. Cui), Avon Foundation (02-2008-081 to X. Cui), Del Webb Foundation (to X. Cui), and the United States Department of Agriculture/Agricultural Research Service under Cooperation Agreement (6250-51000-055 to N.-H. Cheng).

Received for publication March 26, 2010, and accepted in revised form September 29, 2010.

Address correspondence to: Xiaojiang Cui, Department of Molecular Oncology, John Wayne Cancer Institute, Saint John's Health Center, Santa Monica, California 90404, USA. Phone: 310.998.3916; Fax: 310.582.7390; E-mail: cuix@jwci.org. Or to:

Ning-Hui Cheng, Children's Nutrition Research Center, Baylor College of Medicine, Houston, Texas 77030, USA. Phone: 713.798.9326; Fax: 713.798.7101; E-mail: ncheng@bcm.tmc.edu. Or to: Ning Zhang, Center for Basic Medical Sciences, Tianjin Medical University, Tianjin 300070, China. Phone: 86.13502179648; Fax: 86.22.23542068; E-mail: nzhangchina@yahoo.com.

1. Droge W. Free radicals in the physiological control of cell function. *Physiol Rev*. 2002;82(1):47–95.
2. Bergendi L, Benes L, Durackova Z, Ferencik M. Chemistry, physiology and pathology of free radicals. *Life Sci*. 1999;65(18–19):1865–1874.
3. Trachootham D, Lu W, Ogasawara MA, Nilsa RD, Huang P. Redox regulation of cell survival. *Antioxid Redox Signal*. 2008;10(8):1343–1374.
4. Holmgren A, Johansson C, Berndt C, Lonn ME, Hudemann C, Lillig CH. Thiol redox control via thioredoxin and glutaredoxin systems. *Biochem Soc Trans*. 2005;33(pt 6):1375–1377.
5. Kirshner JR, et al. Elesclomol induces cancer cell apoptosis through oxidative stress. *Mol Cancer Ther*. 2008;7(8):2319–2327.
6. Ambrosone CB. Oxidants and antioxidants in breast cancer. *Antioxid Redox Signal*. 2000;2(4):903–917.
7. Mittler R. Oxidative stress, antioxidants and stress tolerance. *Trends Plant Sci*. 2002;7(9):405–410.
8. Halliwell B. Oxidative stress and cancer: have we moved forward? *Biochem J*. 2007;401(1):1–11.
9. Trachootham D, Alexandre J, Huang P. Targeting cancer cells by ROS-mediated mechanisms: a radical therapeutic approach? *Nat Rev Drug Discov*. 2009;8(7):579–591.
10. Reinbothe TM, et al. Glutaredoxin-1 mediates NADPH-dependent stimulation of calcium-dependent insulin secretion. *Mol Endocrinol*. 2009; 23(6):893–900.
11. Aslund F, Beckwith J. Bridge over troubled waters: sensing stress by disulfide bond formation. *Cell*. 1999;96(6):751–753.
12. Holmgren A. Thioredoxin. *Annu Rev Biochem*. 1985; 54:237–271.
13. Muller JM, Rupec RA, Baeuerle PA. Study of gene regulation by NF-kappa B and AP-1 in response to reactive oxygen intermediates. *Methods*. 1997; 11(3):301–312.
14. Powis G, Montfort WR. Properties and biological activities of thioredoxins. *Annu Rev Biophys Biomol Struct*. 2001;30:421–455.
15. Powis G, Kirkpatrick DL. Thioredoxin signaling as a target for cancer therapy. *Curr Opin Pharmacol*. 2007;7(4):392–397.
16. Aslund F, et al. Glutaredoxin-3 from Escherichia coli. Amino acid sequence, 1H AND 15N NMR assignments, and structural analysis. *J Biol Chem*. 1996; 271(12):6736–6745.
17. Holmgren A. Antioxidant function of thioredoxin and glutaredoxin systems. *Antioxid Redox Signal*. 2000;2(4):811–820.
18. Lillig CH, Holmgren A. Thioredoxin and related molecules--from biology to health and disease. *Antioxid Redox Signal*. 2007;9(1):25–47.
19. Mieyal JJ, Gallogly MM, Qanungo S, Sabens EA, Shelton MD. Molecular mechanisms and clinical implications of reversible protein S-glutathionylation. *Antioxid Redox Signal*. 2008;10(11):1941–1988.
20. Peltoniemi MJ, et al. Modulation of glutaredoxin in the lung and sputum of cigarette smokers and chronic obstructive pulmonary disease. *Respir Res*. 2006; 7:133.
21. Urata Y, et al. 17Beta-estradiol protects against oxidative stress-induced cell death through the glutathione/glutaredoxin-dependent redox regulation of Akt in myocardiac H9c2 cells. *J Biol Chem*. 2006; 281(19):13092–13102.
22. Shelton MD, Kern TS, Mieyal JJ. Glutaredoxin regulates nuclear factor kappa-B and intercellular adhesion molecule in Muller cells: model of diabetic retinopathy. *J Biol Chem*. 2007;282(17):12467–12474.
23. Wu WS. The signaling mechanism of ROS in tumor progression. *Cancer Metastasis Rev*. 2006; 25(4):695–705.
24. Husbeck B, Powis G. The redox protein thioredoxin-1 regulates the constitutive and inducible expression of the estrogen metabolizing cytochromes P450 1B1 and 1A1 in MCF-7 human breast cancer cells. *Carcinogenesis*. 2002;23(10):1625–1630.
25. Welsh SJ, Bellamy WT, Briehl MM, Powis G. The redox protein thioredoxin-1 (Trx-1) increases hypoxia-inducible factor 1alpha protein expression: Trx-1 overexpression results in increased vascular endothelial growth factor production and enhanced tumor angiogenesis. *Cancer Res*. 2002; 62(17):5089–5095.
26. Kakolyris S, et al. Thioredoxin expression is associated with lymph node status and prognosis in early operable non-small cell lung cancer. *Clin Cancer Res*. 2001;7(10):3087–3091.
27. Song JJ, Rhee JG, Suntharalingam M, Walsh SA, Spitz DR, Lee YJ. Role of glutaredoxin in metabolic oxidative stress. Glutaredoxin as a sensor of oxidative stress mediated by H2O2. *J Biol Chem*. 2002; 277(48):46566–46575.
28. Creighton CJ, et al. Insulin-like growth factor-I activates gene transcription programs strongly associated with poor breast cancer prognosis. *J Clin Oncol*. 2008;26(25):4078–4085.
29. Witte S, Villalba M, Bi K, Liu Y, Isakov N, Altman A. Inhibition of the c-Jun N-terminal kinase/AP-1 and NF-kappaB pathways by PICOT, a novel protein kinase C-interacting protein with a thioredoxin homology domain. *J Biol Chem*. 2000;275(3):1902–1909.
30. Lillig CH, Berndt C, Holmgren A. Glutaredoxin systems. *Biochim Biophys Acta*. 2008;1780(11):1304–1317.
31. Pujol-Carrion N, Belli G, Herrero E, Nogues A, de la Torre-Ruiz MA. Glutaredoxins Grx3 and Grx4 regulate nuclear localisation of Aft1 and the oxidative stress response in Saccharomyces cerevisiae. *J Cell Sci*. 2006;119(pt 21):4554–4564.
32. Jeong D, et al. PICOT inhibits cardiac hypertrophy and enhances ventricular function and cardiomyocyte contractility. *Circ Res*. 2006;99(3):307–314.
33. Kato N, Motohashi S, Okada T, Ozawa T, Mashima K. PICOT, protein kinase C theta-interacting protein, is a novel regulator of FcepsilonRI-mediated mast cell activation. *Cell Immunol*. 2008;251(1):62–67.
34. Cha H, et al. PICOT is a critical regulator of cardiac hypertrophy and cardiomyocyte contractility. *J Mol Cell Cardiol*. 2008;45(6):796–803.
35. Richardson AL, et al. X chromosomal abnormalities in basal-like human breast cancer. *Cancer Cell*. 2006;9(2):121–132.
36. Landi MT, et al. Gene expression signature of cigarette smoking and its role in lung adenocarcinoma development and survival. *PLoS One*. 2008;3(2):e1651.
37. Ki DH, et al. Whole genome analysis for liver metastasis gene signatures in colorectal cancer. *Int J Cancer*. 2007;121(9):2005–2012.
38. Chen X, et al. Variation in gene expression patterns in human gastric cancers. *Mol Biol Cell*. 2003; 14(8):3208–3215.
39. Dyrskjot L, et al. Gene expression in the urinary bladder: a common carcinoma in situ gene expression signature exists disregarding histopathological classification. *Cancer Res*. 2004;64(11):4040–4048.
40. Pyeon D, et al. Fundamental differences in cell cycle deregulation in human papillomavirus-positive and human papillomavirus-negative head/neck and cervical cancers. *Cancer Res*. 2007;67(10):4605–4619.
41. Hall A. Ras-related GTPases and the cytoskeleton. *Mol Biol Cell*. 1992;3(5):475–479.
42. Eck SM, Hoopes PJ, Petrella BL, Coon CI, Brinckerhoff CE. Matrix metalloproteinase-1 promotes breast cancer angiogenesis and osteolysis in a novel in vivo model. *Breast Cancer Res Treat*. 2009;116(1):79–90.
43. Streicher KL, Willmarth NE, Garcia J, Boerner JL, Dewey TG, Ethier SP. Activation of a nuclear factor kappaB/interleukin-1 positive feedback loop by amphiregulin in human breast cancer cells. *Mol Cancer Res*. 2007;5(8):847–861.
44. Kosower NS, Kosower EM. The glutathione status of cells. *Int Rev Cytol*. 1978;54:109–160.
45. Kirlin WG, Cai J, Thompson SA, Diaz D, Kavanagh TJ, Jones DP. Glutathione redox potential in response to differentiation and enzyme inducers. *Free Radic Biol Med*. 1999;27(11–12):1208–1218.
46. Jiang B, Haverty M, Brecher P. N-acetyl-L-cysteine enhances interleukin-1beta-induced nitric oxide synthase expression. *Hypertension*. 1999; 34(4 pt 1):574–579.
47. Perkins ND. The Rel/NF-kappa B family: friend and foe. *Trends Biochem Sci*. 2000;25(9):434–440.
48. Pahl HL. Activators and target genes of Rel/NF-kappaB transcription factors. *Oncogene*. 1999; 18(49):6853–6866.
49. Hiscott J, et al. Characterization of a functional NF-kappa B site in the human interleukin 1 beta promoter: evidence for a positive autoregulatory loop. *Mol Cell Biol*. 1993;13(10):6231–6240.
50. Das DK, Maulik N. Conversion of death signal into survival signal by redox signaling. *Biochemistry (Mosc)*. 2004;69(1):10–17.
51. Montagut C, et al. Activation of nuclear factor-kappa B is linked to resistance to neoadjuvant chemotherapy in breast cancer patients. *Endocr Relat Cancer*. 2006;13(2):607–616.
52. Biswas DK, et al. NF-kappa B activation in human breast cancer specimens and its role in cell proliferation and apoptosis. *Proc Natl Acad Sci U S A*. 2004; 101(27):10137–10142.
53. Reynaert NL, et al. Dynamic redox control of NF-kappaB through glutaredoxin-regulated S-glutathionylation of inhibitory kappaB kinase beta. *Proc Natl Acad Sci U S A*. 2006;103(35):13086–13091.
54. Zandi E, Chen Y, Karin M. Direct phosphorylation of IkappaB by IKKalpha and IKKbeta: discrimination between free and NF-kappaB-bound substrate. *Science*. 1998;281(5381):1360–1363.
55. Viatour P, Merville MP, Bours V, Chariot A. Phosphorylation of NF-kappaB and IkappaB proteins: implications in cancer and inflammation. *Trends Biochem Sci*. 2005;30(1):43–52.
56. Sen CK, Packer L. Antioxidant and redox regulation of gene transcription. *FASEB J*. 1996;10(7):709–720.
57. Droge W, et al. Functions of glutathione and glutathione disulfide in immunology and immunopathology. *FASEB J*. 1994;8(14):1131–1138.
58. Huber MA, et al. NF-kappaB is essential for epithelial-mesenchymal transition and metastasis in a model of breast cancer progression. *J Clin Invest*. 2004;114(4):569–581.
59. Hong KO, et al. Inhibition of Akt activity induces the mesenchymal-to-epithelial reverting transition with restoring E-cadherin expression in KB and KOSCC-25B oral squamous cell carcinoma cells. *J Exp Clin Cancer Res*. 2009;28:28.
60. Meng F, Liu L, Chin PC, D'Mello SR. Akt is a downstream target of NF-kappa B. *J Biol Chem*. 2002; 277(33):29674–29680.
61. Finco TS, Westwick JK, Norris JL, Beg AA, Der CJ, Baldwin AS Jr. Oncogenic Ha-Ras-induced signaling activates NF-kappaB transcriptional activity, which is required for cellular transformation. *J Biol Chem*. 1997;272(39):24113–24116.
62. Minn AJ, et al. Distinct organ-specific metastatic potential of individual breast cancer cells and primary tumors. *J Clin Invest*. 2005;115(1):44–55.

63. Bos PD, et al. Genes that mediate breast cancer metastasis to the brain. *Nature*. 2009;459(7249):1005–1009.
64. Pawitan Y, et al. Gene expression profiling spares early breast cancer patients from adjuvant therapy: derived and validated in two population-based cohorts. *Breast Cancer Res*. 2005;7(6):R953–R964.
65. Sotiriou C, et al. Gene expression profiling in breast cancer: understanding the molecular basis of histologic grade to improve prognosis. *J Natl Cancer Inst*. 2006;98(4):262–272.
66. Cha MK, Kim IH. Preferential overexpression of glutaredoxin3 in human colon and lung carcinoma. *Cancer Epidemiol*. 2009;33(3–4):281–287.
67. Valko M, Rhodes CJ, Moncol J, Izakovic M, Mazur M. Free radicals, metals and antioxidants in oxidative stress-induced cancer. *Chem Biol Interact*. 2006;160(1):1–40.
68. Gibson LM, Dingra NN, Outten CE, Lebioda L. Structure of the thioredoxin-like domain of yeast glutaredoxin 3. *Acta Crystallogr D Biol Crystallogr*. 2008; 64(pt 9):927–932.
69. Haunhorst P, Berndt C, Eitner S, Godoy JR, Lillig CH. Characterization of the human monothiol glutaredoxin 3 (PICOT) as iron-sulfur protein. *Biochem Biophys Res Commun*. 2010;394(2):372–376.
70. Sovak MA, et al. Aberrant nuclear factor-kappaB/Rel expression and the pathogenesis of breast cancer. *J Clin Invest*. 1997;100(12):2952–2960.
71. Dejardin E, Bonizzi G, Bellahcene A, Castronovo V, Merville MP, Bours V. Highly-expressed p100/p52 (NFKB2) sequesters other NF-kappa B-related proteins in the cytoplasm of human breast cancer cells. *Oncogene*. 1995;11(9):1835–1841.
72. Rayet B, Gelinas C. Aberrant rel/nfkb genes and activity in human cancer. *Oncogene*. 1999; 18(49):6938–6947.
73. Ritter N, Mussig E, Steinberg T, Kohl A, Komposch G, Tomakidi P. Elevated expression of genes assigned to NF-kappaB and apoptotic pathways in human periodontal ligament fibroblasts following mechanical stretch. *Cell Tissue Res*. 2007;328(3):537–548.
74. Ghandhi SA, Yaghoubian B, Amundson SA. Global gene expression analyses of bystander and alpha particle irradiated normal human lung fibroblasts: synchronous and differential responses. *BMC Med Genomics*. 2008;1:63.
75. Ferri N, Garton KJ, Raines EW. An NF-kappaB-dependent transcriptional program is required for collagen remodeling by human smooth muscle cells. *J Biol Chem*. 2003;278(22):19757–19764.
76. Poola I, DeWitty RL, Marshalleck JJ, Bhatnagar R, Abraham J, Leffall LD. Identification of MMP-1 as a putative breast cancer predictive marker by global gene expression analysis. *Nat Med*. 2005;11(5):481–483.
77. Kang Y, et al. A multigenic program mediating breast cancer metastasis to bone. *Cancer Cell*. 2003; 3(6):537–549.
78. Minn AJ, et al. Genes that mediate breast cancer metastasis to lung. *Nature*. 2005;436(7050):518–524.
79. Nash KT, Welch DR. The KISS1 metastasis suppressor: mechanistic insights and clinical utility. *Front Biosci*. 2006;11:647–659.
80. Min C, Eddy SF, Sherr DH, Sonenshein GE. NF-kappaB and epithelial to mesenchymal transition of cancer. *J Cell Biochem*. 2008;104(3):733–744.
81. Wang X, et al. Oestrogen signalling inhibits invasive phenotype by repressing RelB and its target BCL2. *Nat Cell Biol*. 2007;9(4):470–478.
82. Luo JL, Kamata H, Karin M. IKK/NF-kappaB signaling: balancing life and death--a new approach to cancer therapy. *J Clin Invest*. 2005;115(10):2625–2632.
83. Klatt P, Lamas S. Regulation of protein function by S-glutathiolation in response to oxidative and nitrosative stress. *Eur J Biochem*. 2000;267(16):4928–4944.
84. Jones DP. Radical-free biology of oxidative stress. *Am J Physiol Cell Physiol*. 2008;295(4):C849–868.
85. Kabe Y, Ando K, Hirao S, Yoshida M, Handa H. Redox regulation of NF-kappaB activation: distinct redox regulation between the cytoplasm and the nucleus. *Antioxid Redox Signal*. 2005;7(3–4):395–403.
86. Qanungo S, Starke DW, Pai HV, Mieyal JJ, Nieminen AL. Glutathione supplementation potentiates hypoxic apoptosis by S-glutathionylation of p65-NFkappaB. *J Biol Chem*. 2007;282(25):18427–18436.
87. Alisi A, et al. Glutathionylation of p65NF-kappaB correlates with proliferating/apoptotic hepatoma cells exposed to pro- and anti-oxidants. *Int J Mol Med*. 2009;24(3):319–326.
88. Jones DP. Redefining oxidative stress. *Antioxid Redox Signal*. 2006;8(9–10):1865–1879.
89. Schumacker PT. Reactive oxygen species in cancer cells: live by the sword, die by the sword. *Cancer Cell*. 2006;10(3):175–176.
90. Trachootham D, et al. Selective killing of oncogenically transformed cells through a ROS-mediated mechanism by beta-phenylethyl isothiocyanate. *Cancer Cell*. 2006;10(3):241–252.
91. Oh SY, et al. Selective cell death of oncogenic Akt-transduced brain cancer cells by etoposide through reactive oxygen species mediated damage. *Mol Cancer Ther*. 2007;6(8):2178–2187.
92. Qu Y, et al. Elesclomol, counteracted by Akt survival signaling, enhances the apoptotic effect of chemotherapy drugs in breast cancer cells. *Breast Cancer Res Treat*. 2010;121(2):311–321.
93. Madrid LV, Mayo MW, Reuther JY, Baldwin AS Jr. Akt stimulates the transactivation potential of the RelA/p65 Subunit of NF-kappa B through utilization of the Ikappa B kinase and activation of the mitogen-activated protein kinase p38. *J Biol Chem*. 2001; 276(22):18934–18940.
94. Aggarwal BB, Shishodia S, Sandur SK, Pandey MK, Sethi G. Inflammation and cancer: how hot is the link? *Biochem Pharmacol*. 2006;72(11):1605–1621.
95. Levine L, et al. Bombesin stimulates nuclear factor kappa B activation and expression of proangiogenic factors in prostate cancer cells. *Cancer Res*. 2003; 63(13):3495–3502.
96. Harvey JM, Clark GM, Osborne CK, Allred DC. Estrogen receptor status by immunohistochemistry is superior to the ligand-binding assay for predicting response to adjuvant endocrine therapy in breast cancer. *J Clin Oncol*. 1999;17(5):1474–1481.